

ON THE STRUCTURE OF THE LOWER TROPOSPHERE: JULY 2001 NEAR 120W AND 30N

Bjorn Stevens*, Anton Beljaars†, Simona Bordonì*, Christopher Holloway*, Martin Köhler†, Steven Krueger‡, Verica Savic-Jovic* and Yunyan Zhang*

* UCLA, † ECMWF, ‡ UU

(verica@atmos.ucla.edu)

Introduction

The state of the lower troposphere in the region with prevailing stratocumulus is studied by employing the routine data, embodied by the available reanalysis, satellite and monitoring data, over the remote marine environment sampled during DYCOMS-II, as well as the directly measured data. In particular, we ask: given the routine data, how well could we have inferred the basic state of the lower troposphere had we not been there to measure it directly? To the extent routine data products provide an adequate representation of the lower troposphere observed during DYCOMS-II we ask further: to what extent were conditions during DYCOMS-II typical of past years? Or in turn, to what extent is the inter-annual variability of data records that reproduced the DYCOMS-II observations consistent with past studies? Our principal goal is to develop a clearer picture of the state of the lower troposphere in the heart of the stratocumulus regime, as well as the subset of routinely available data capable of representing it with reasonable fidelity on timescales pertinent to the processes which motivate much of our ultimate interest in this cloud regime.

Data

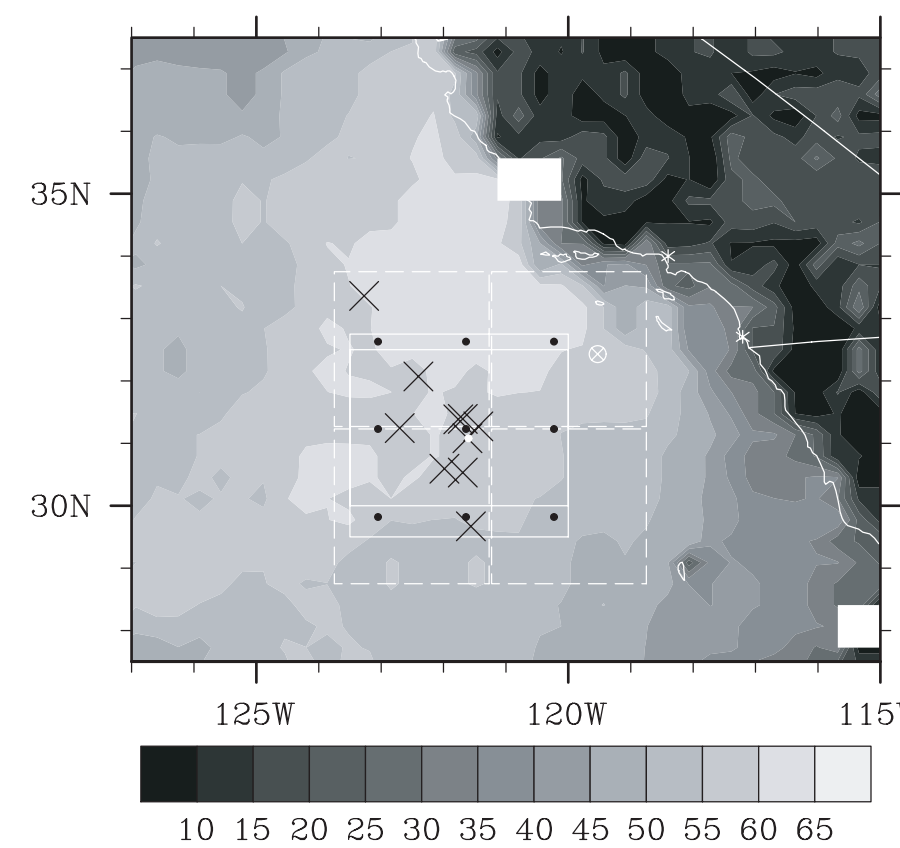


Figure 1: Analysis area shown boxed over the mean 1500-2100 UTC (800-1400 PDT) visible reflectivity from the ISCCP DX data. Center of flight operations of each of the 10 flights is shown by X's. The position of the nearest monitoring buoy is shown by the circled x.

The analysis is based on data from a variety of sources, with the primary source of actual state being the AIR-CRAFT data. In addition to standard measurements these include specialized measurements from DROP-SONDES, downward-looking LIDAR and downward-looking PYRANOMETER.

SATELLITE-retrieved fields include: visual images of cloud coverage from GOES-10; cloud climatological data from the ISCCP DX archive; surface winds from QuikSCAT; column water vapor, column liquid water, SSTs and surface winds from TMI; secondary estimates of column water vapor and column liquid water from AMSU-A.

We also use the ERA-40 (full T159 ECMWF product) and NCEP REANALYSES, as well as FORECAST products for the DYCOMS-II region from ECMWF (IFS) and NCEP (GFS). The IFS products are the area-average at 60 σ levels at hourly intervals from the 72-hour forecasts initializing at 12 UTC, while the GFS are the nine-grid points average at 40 σ levels from 48-hour forecasts beginning at 00 UTC.

Synoptic Overview

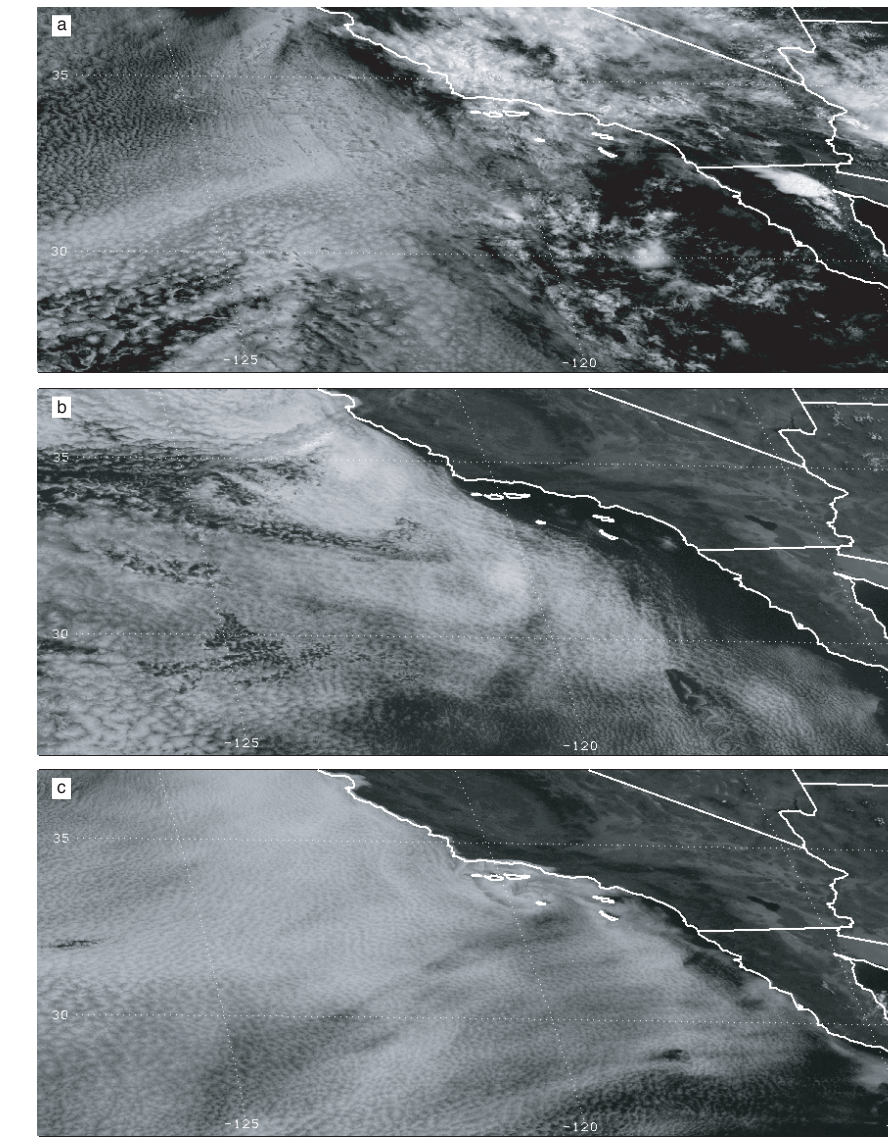


Figure 2: Channel 1 (visible) reflectivity from GOES 10 at 1800 UTC on: July 6th (a); July 12th (b); and 27th (c).

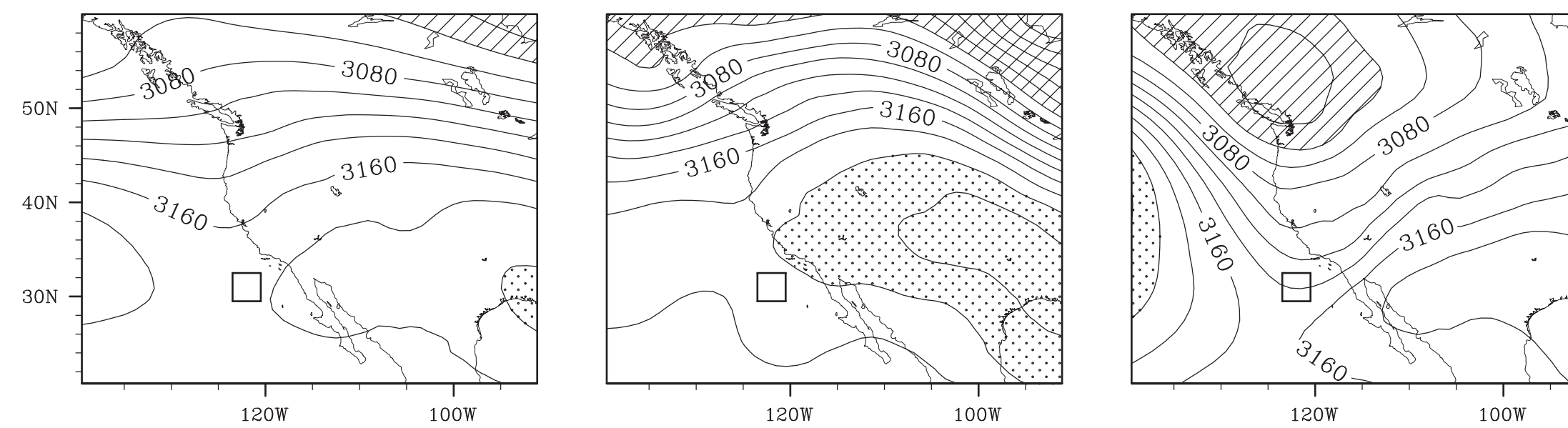


Figure 4: 700 hPa geopotential height, Φ_{700} as derived from the ERA40: Long-term July Climatology (left panel); July 3-5 (middle); July 15-17 (right). Stippling indicates regions of high pressures ($\Phi_{700} > 3200$ m), hatching indicates regions of low pressure ($\Phi_{700} < 3040$ m). Contours every 20 m, and study region indicated by box.

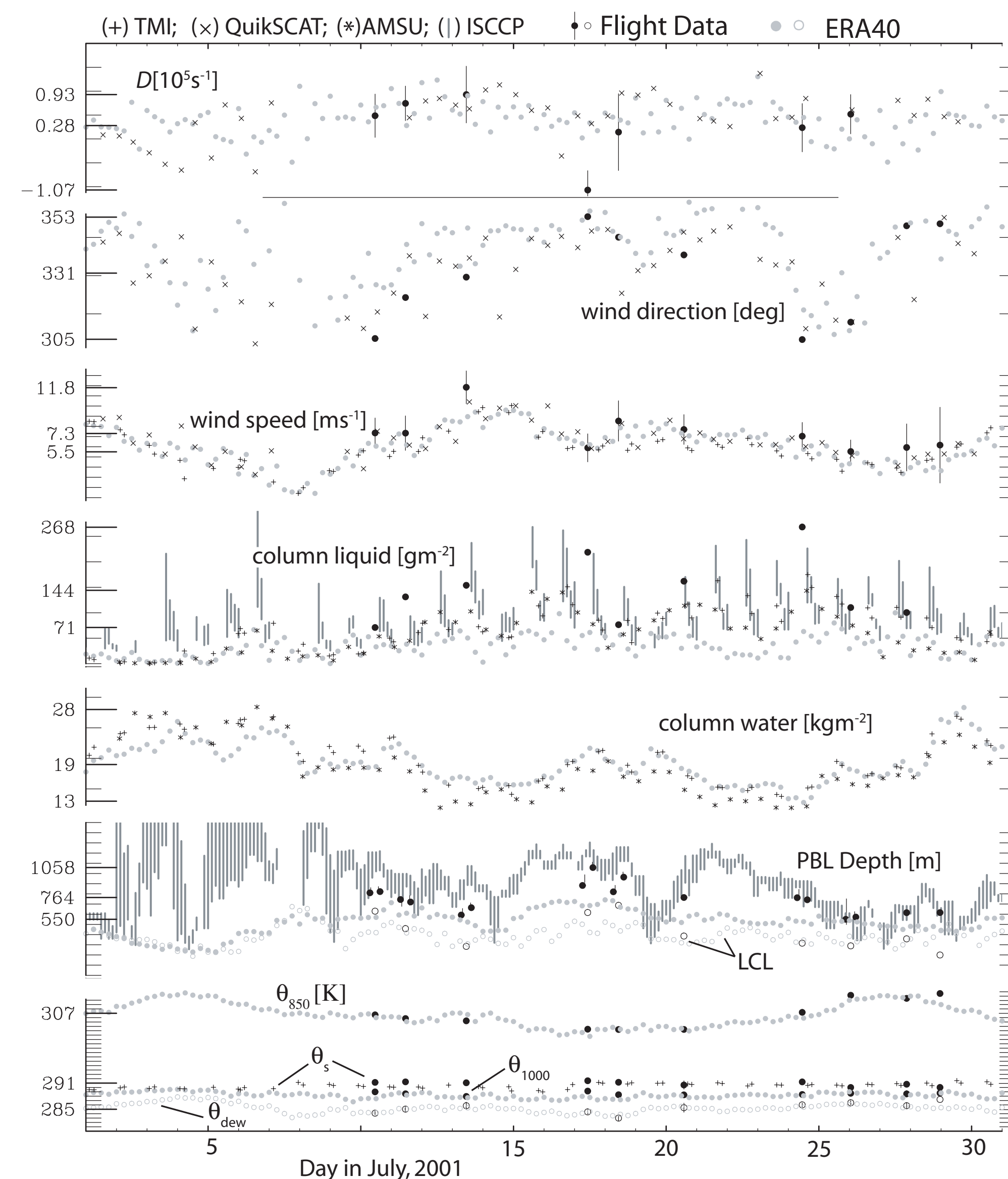


Figure 3: Synthesis of flight and routine data over study area for July, 2001. Estimates of variability accompany the flight data, open circles in bottom panel denote θ_{LCL} , and open circles in second panel from bottom denote LCL. For reasons of clarity the NCEP data are not included in this plot.

'Routine' Analysis

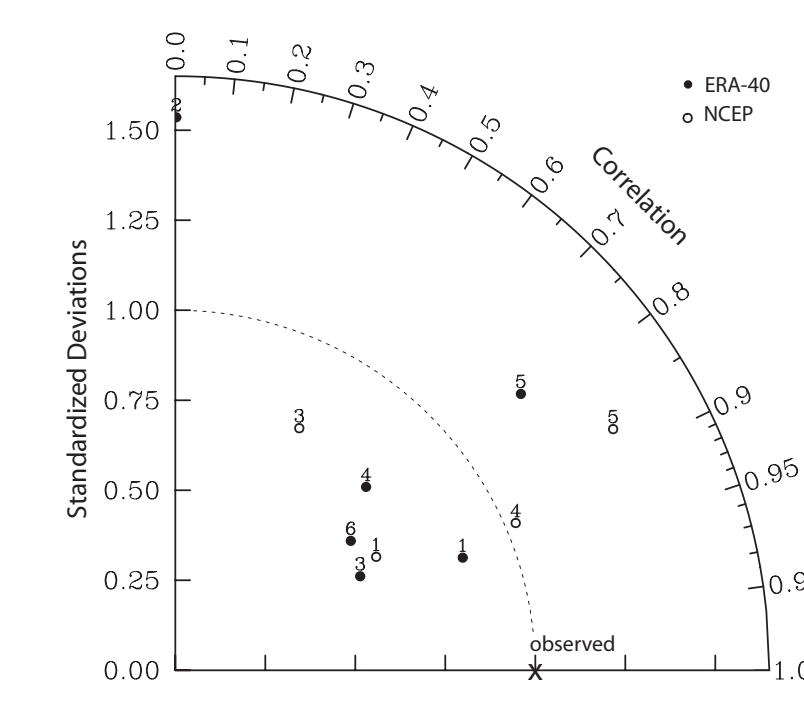


Figure 5: Taylor diagram illustrating the correspondence between routine (ERA-40 and NCEP) and flight data. (1) θ_{850} ; (2) θ_m ; (3) q_m ; (4) u_m ; (5) v_m ; (6) PBL depth.

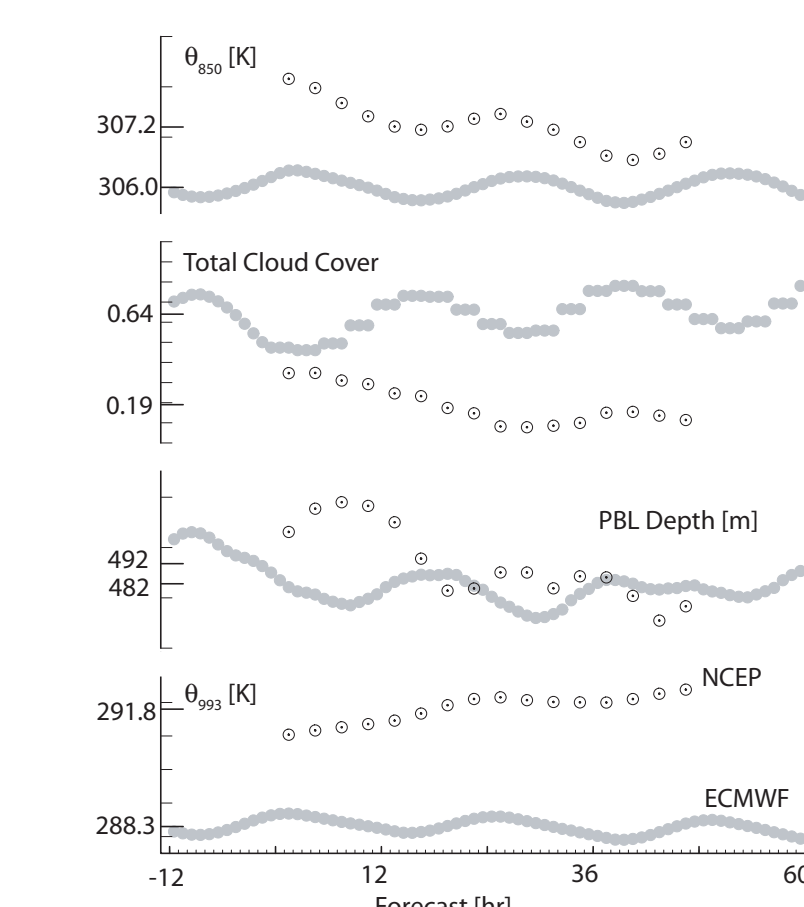


Figure 7: July average at each forecast hour for selected fields from ECMWF (grey circles) and NCEP (open circle with center dot). From top to bottom: θ_{850} , total cloud cover, PBL depth, and θ_{993} .

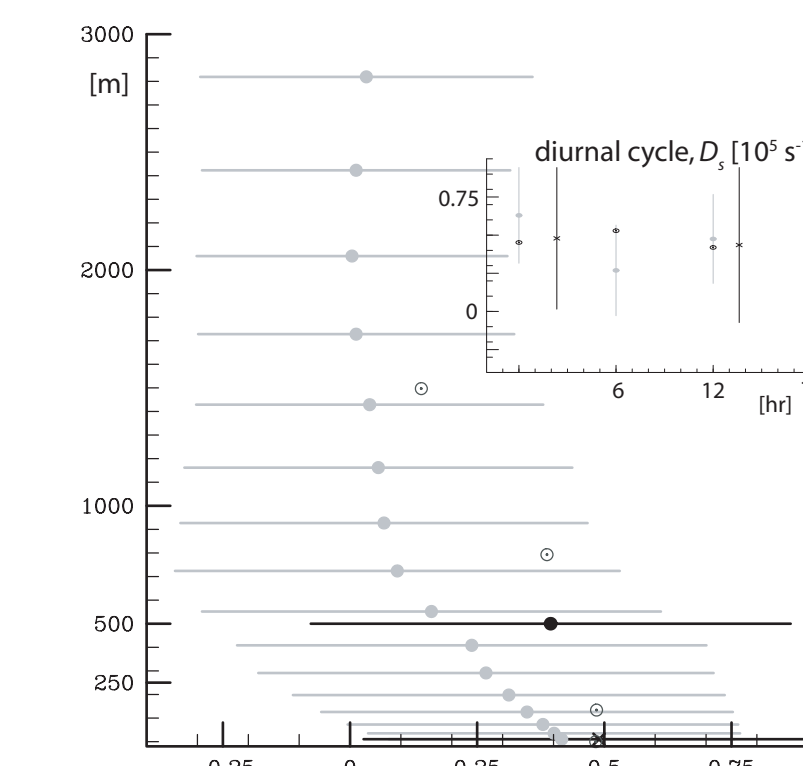


Figure 6: Vertical profile of divergence averaged for all available July 2001 data from ERA-40 (grey solid dots), NCEP (open circles with center dot), Flight data (black solid dot), and QuikSCAT (cross). Diurnal cycle showing D_s at different analysis times and the ascending and descending QuikSCAT measurements shown in inset. Standard deviations from NCEP estimates not shown, but typically 2-5 times larger than those from ERA-40.

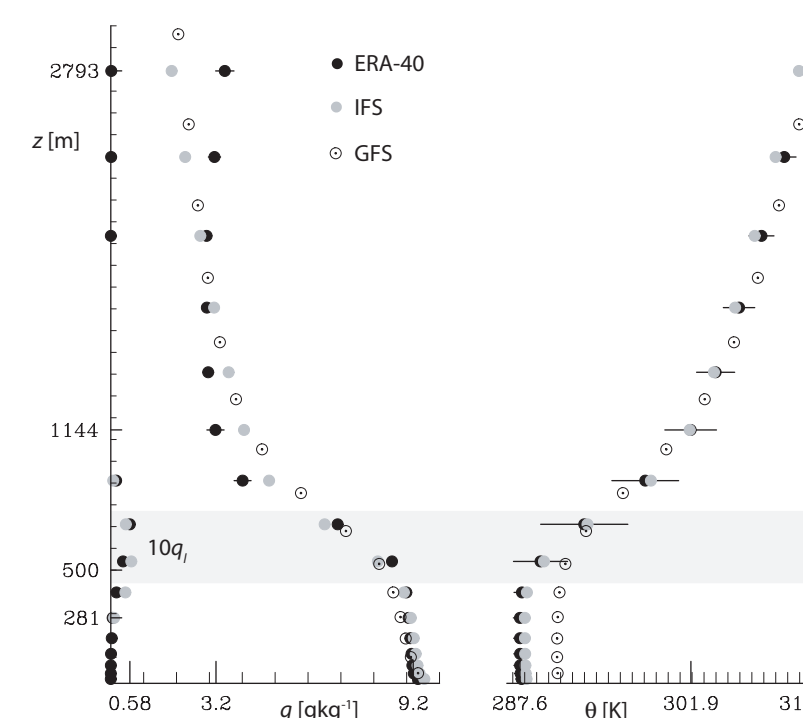


Figure 8: Mean profile for July 10-20 2001, for ERA-40, GFS and IFS 0000-2400 UTC forecasts. For guidance the position of the observed cloud layer is indicated by the shading.

Conclusions

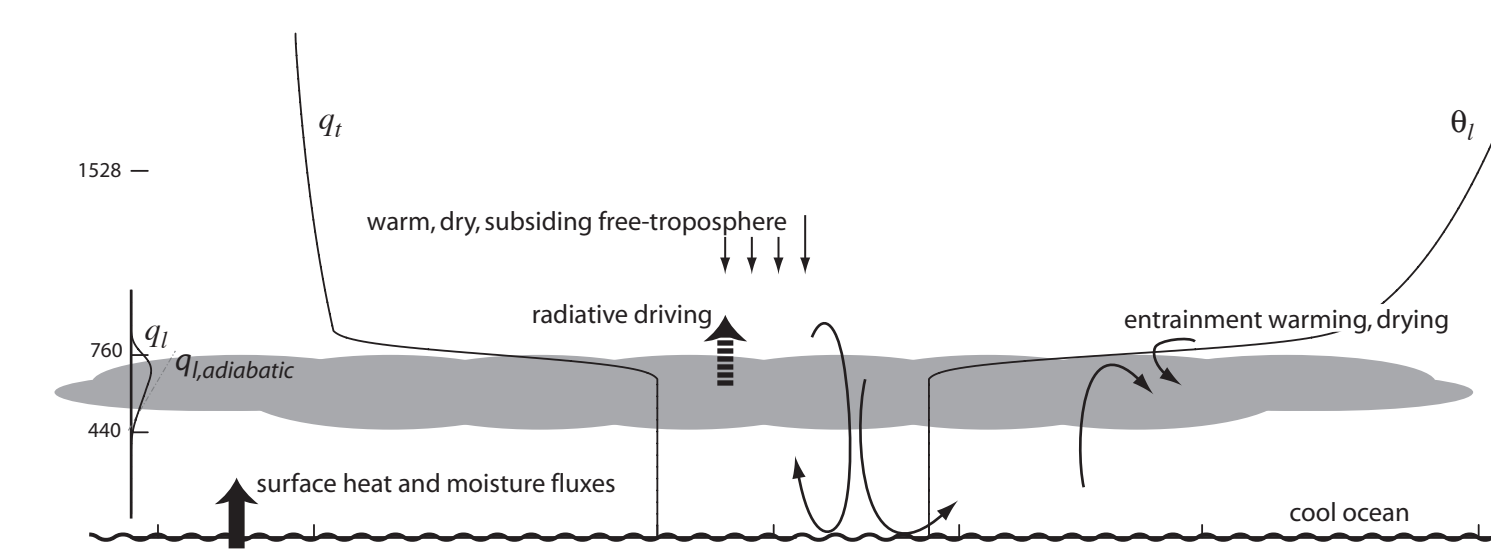


Figure 12: Sketch of mean thermodynamics structure of lower troposphere, for July 2001, near 120W 30N. The potential temperature, specific humidity and height at 850 hPa are indicated, as are values within and just above the STBL.

The ISCCP data product provides very useful insights into the structure of the observed PBL.

The ERA-40 reanalysis, as well as IFS which underlies it, admirably reproduce the structure of the environment around the STBL.

The chief deficiencies of both the IFS and ERA-40 are in its representation of the STBL itself, many of which can be tied to the method for diagnosing the STBL depth in the IFS. Recent efforts to incorporate moist processes in the formulation of the IFS boundary layer model have led to marked improvements. Because of its better performances than the NCEP reanalysis, we believe the ERA-40 to be the more useful product at this time.

The most striking finding to arise from this study is that the inter-annual correlation between lower tropospheric stability and cloud amount at Ocean Weather Ship N does not hold broadly across the region. This highlights the difficulty of making climate observations from fixed spatial locations, even over the open ocean.

Typical July?

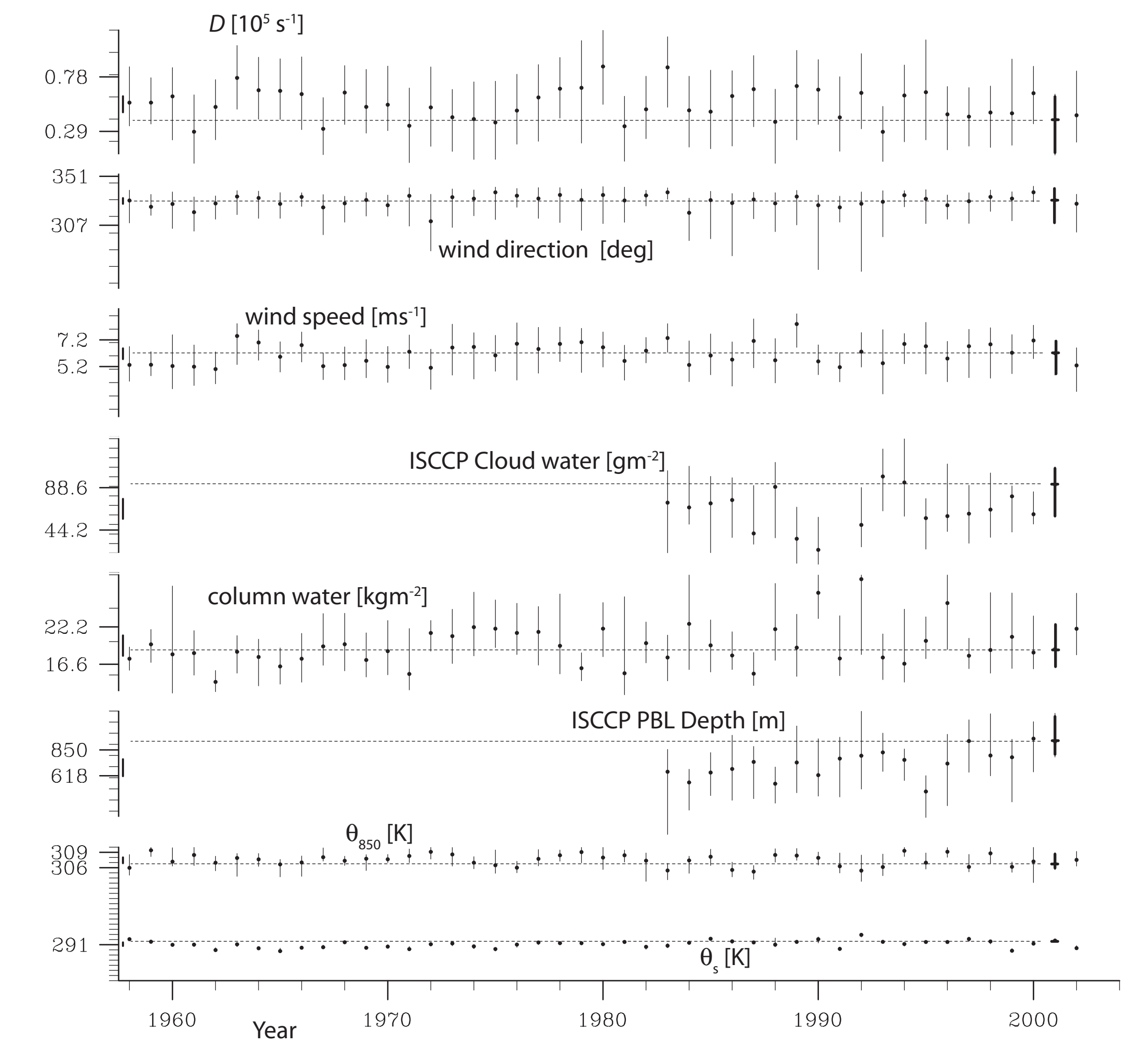


Figure 9: Summary of year-to-year variability in July following the format of Fig. 3. Data for 2001 are thickened and used as a reference for the dashed base lines.

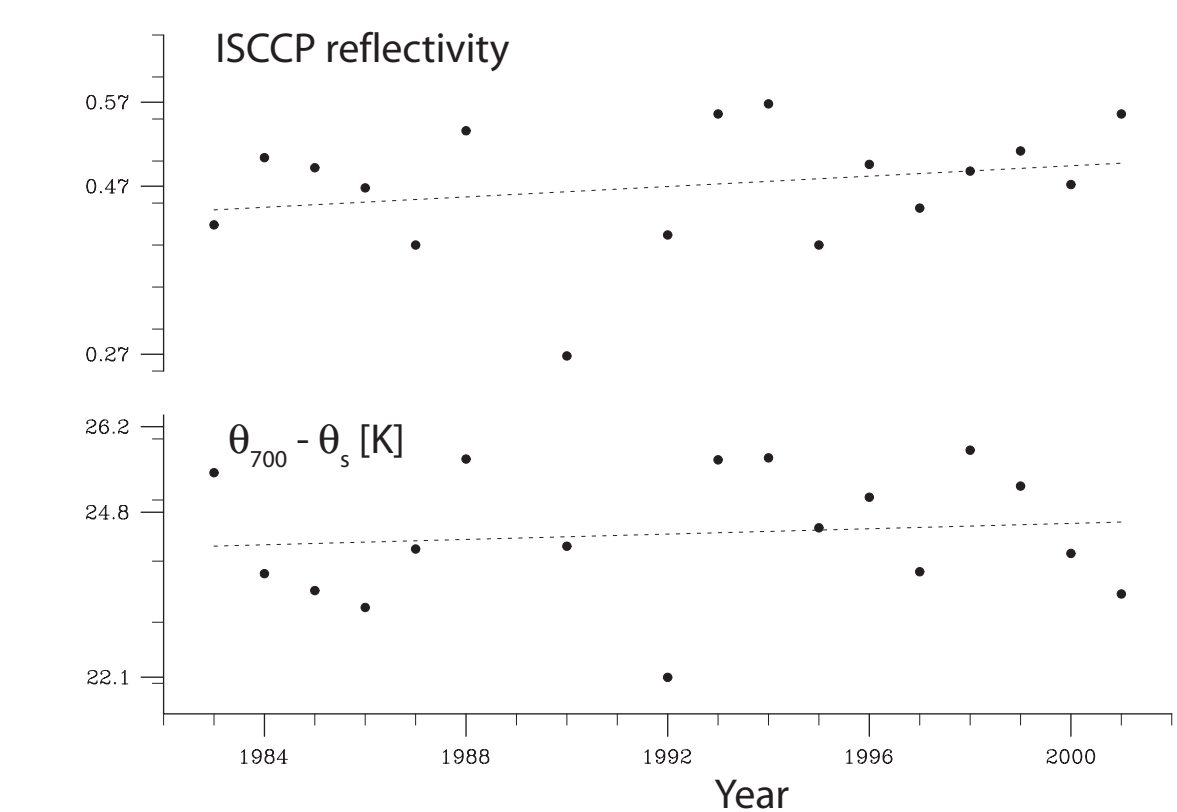


Figure 10: ISCCP daytime cloud reflectivity (left); lower tropospheric (700 hPa) stability (right). Julys for which the ISCCP record has fewer than ten days of data over our study region are excluded from the record.

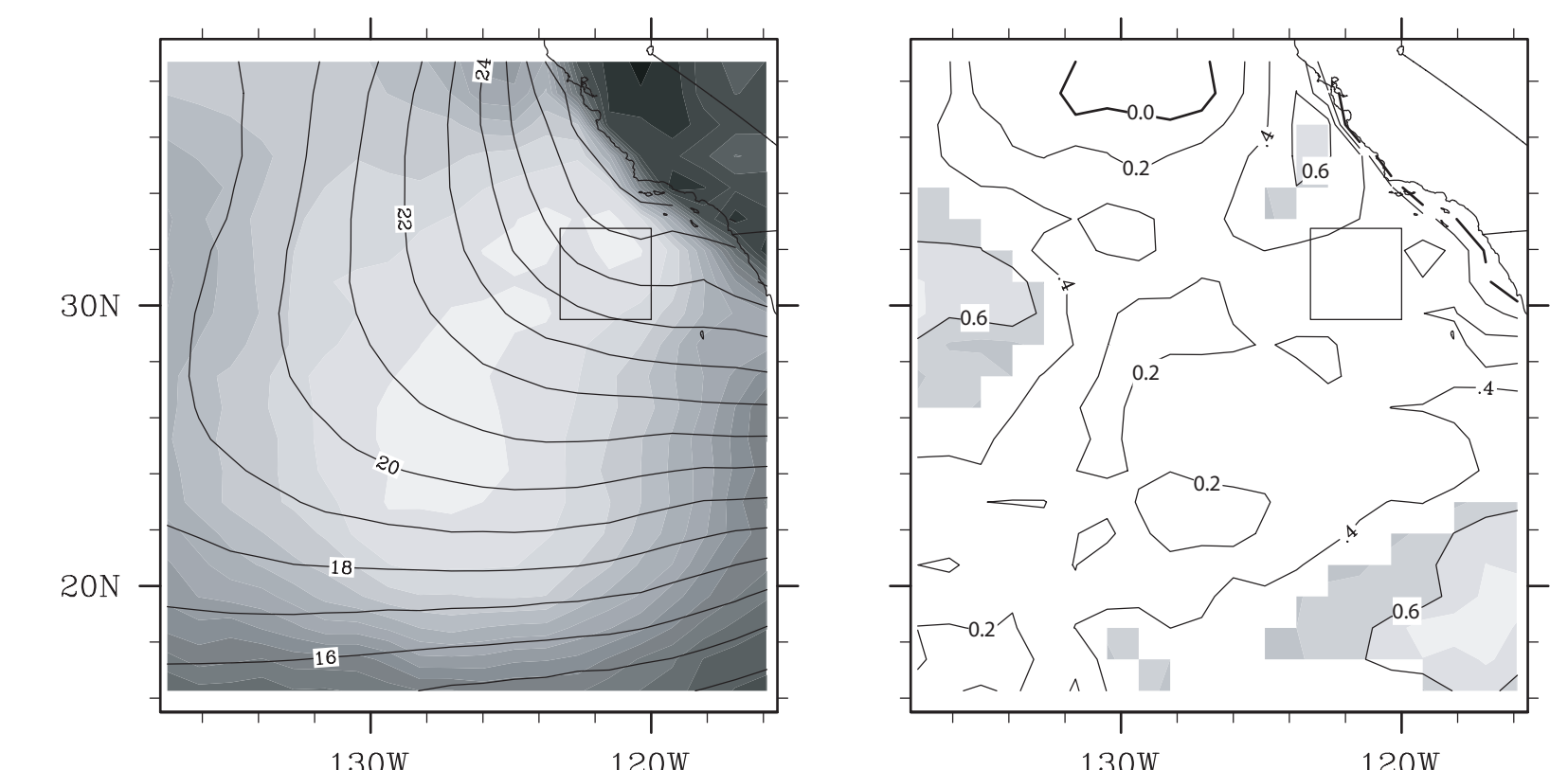


Figure 11: Lower tropospheric stability and ISCCP daytime cloud reflectivity (left); inter-annual correlation coefficient between these two fields (right).

Acknowledgments

ECMWF ERA-40 data have been obtained from a variety of locations, including the ECMWF data server, and from the data systems section at the NCAR. NCEP Reanalysis data provided by the NOAA-CIRES Climate Diagnostics Center, Boulder, Colorado, USA (<http://www.cdc.noaa.gov>). The ISCCP DX data were obtained from the International Satellite Cloud Climatology Project data archives maintained by the NASA DAAC. The QuikSCAT Level 3 Ocean Wind Vector data are obtained from the Physical Oceanography Distributed Active Archive Center (PO.DAAC) at NASA JPL in Pasadena, CA (<http://podaac.jpl.nasa.gov>). TMI data are produced by Remote Sensing Systems and sponsored by the NASA Earth Science REASoN DISCOVER Project (<http://www.remss.com>). GOES-10 data are available at Science and Engineering Data Center (<http://www.ssec.wisc.edu/datacenter/>). This work was supported by NASA through Fellowship NGT530499 and Grand NAG512559.